

A link between measured neutron star masses and lattice QCD data

Ignazio Bombaci^a, Domenico Logoteta^b

^a*Dipartimento di Fisica “E. Fermi”, Università di Pisa, and INFN, Sezione di Pisa, Largo B. Pontecorvo, 3 I-56127 Pisa, Italy*

^b*Centro de Física Computacional, Department of Physics, University of Coimbra, 3004-516 Coimbra, Portugal*

Abstract

We study the hadron–quark phase transition in neutron star matter and the structural properties of hybrid stars using an equation of state (EOS) for the quark phase derived with the Field Correlator Method (FCM). We make use of measured neutron star masses, and particularly the mass of PSR J1614-2230, to constrain the values of the gluon condensate G_2 which is one of the EOS parameter within the FCM. We find that the values of G_2 extracted from the mass measurement of PSR J1614-2230 are fully consistent with the values of the same quantity derived, within the FCM, from recent lattice QCD calculations of the deconfinement transition temperature at zero baryon chemical potential. The FCM thus provides a powerful tool to link numerical calculations of QCD on a space-time lattice with neutron stars physics.

Key words: dense matter, elementary particles, Stars: neutron PACS 26.60.+c, 25.75.Nq, 97.60.Jd

1. Introduction

Neutron stars, the compact remnants of supernova explosions, are unique natural laboratories to explore the phase diagram of quantum chromodynamics (QCD) in the low temperature T and high baryon chemical potential μ_b region [1,2]. In this regime nonperturbative aspects of QCD are expected to play a crucial role, and a transition to a phase with deconfined quarks and gluons is expected to occur and to influence a number of interesting astrophysical phenomena [3–9].

Recent high precision numerical calculations of QCD on a space-time lattice at $\mu_b = 0$ (*i.e.* zero baryon density) have shown that at high temperature and for physical values of the quark masses, the transition to quark gluon plasma is a crossover [10] rather than a real phase transition.

Unfortunately, present lattice QCD calculations at finite baryon chemical potential are unrealizable by all presently known lattice methods (see *e.g.* [11]). Thus, to explore the QCD

phase diagram at low T and high μ_b , it is necessary to invoke some approximations in QCD or to apply some QCD effective model.

Along these lines, different models of the equation of state (EOS) of quark matter, as the bag model [12] or the Nambu Jona-Lasinio (NJL) model [13,14], have been intensively used by many authors to calculate the structure of strange stars [15–17], or the structure of the so called hybrid stars, *i.e.* neutron stars with a quark matter core. These EOS models are expected to be reasonable at very large density, but they crumbles in the density region where quarks clusterize to form hadrons, *i.e.* in the region where the deconfinement phase transition takes place. In addition, the bag model and the NJL model, as other QCD effective models, can not make predictions in the high T and zero μ_b region, and thus can not be tested using present lattice QCD calculations.

Recently the deconfinement phase transition has been described using an EOS of quark gluon plasma derived within the Field Correlator Method (FCM) [18,19] extended to finite baryon chemical potential [20–22]. The FCM

is a nonperturbative approach to QCD which includes from first principles the dynamics of confinement. The model is parameterized in terms of the gluon condensate G_2 and the large distance static quark-antiquark ($Q\bar{Q}$) potential V_1 . These two quantities control the EOS of the deconfined phase at fixed quark masses and temperature. The main constructive characteristic of the FCM is the possibility to describe the whole QCD phase diagram as it can span from high temperature and low baryon chemical potential, to low T and high μ_b limit [20–22].

A very interesting feature of the FCM is that the value of the gluon condensate can be obtained from lattice QCD calculations of the deconfinement transition temperature T_c , at zero baryon chemical potential. Thus we have an efficacious tool to directly link lattice QCD simulations and neutron star physics.

To explore this link is the main purpose of the present work. In particular, we will investigate the possibility for the occurrence of the quark deconfinement transition in neutron stars and the possibility to have stable hybrid star configurations using the FCM for the quark phase EOS and a relativistic mean field model [23] for the EOS of the hadronic phase.

2. EOS of the Quark Phase

The quark matter equation of state we used in this work is based on the Field Correlator Method [18,19]. Recently this method has been extended to the case of nonzero baryon density [20–22] making possible its application to neutron star matter.

The main advantage of the FCM is a natural explanation and treatment of the dynamics of confinement in terms of Color Electric $D^E(x)$, $D_1^E(x)$ and Color Magnetic $D^H(x)$, $D_1^H(x)$ gaussian correlators [19].

D^E contributes to the standard string tension σ^E through [20]:

$$\sigma^E = \frac{1}{2} \int D^E(x) d^2x. \quad (1)$$

The string tension σ^E vanishes as D^E goes to zero at $T \geq T_c$ [20], and this leads to deconfinement. The correlators have been calculated on the lattice [24] and also analytically [25].

Within the FCM the quark pressure P_q , for a single flavour, read [20]:

$$P_q/T^4 = \frac{1}{\pi^2} [\phi_\nu(\frac{\mu_q - V_1/2}{T}) + \phi_\nu(-\frac{\mu_q + V_1/2}{T})] \quad (2)$$

where

$$\phi_\nu(a) = \int_0^\infty du \frac{u^4}{\sqrt{u^2 + \nu^2}} \frac{1}{(\exp[\sqrt{u^2 + \nu^2} - a] + 1)}, \quad (3)$$

$\nu = m_q/T$ and V_1 is the large distance static $Q\bar{Q}$ potential:

$$V_1(T) = \int_0^{1/T} d\tau (1 - \tau T) \int_0^\infty d\chi \chi D_1^E(\sqrt{\chi^2 + \tau^2}). \quad (4)$$

The nonperturbative contribution to $D_1^E(x)$ is parametrised as [19]:

$$D_1^E(x) = D_1^E(0) \exp(-|x|/\lambda) \quad (5)$$

where λ is the vacuum correlation length. Following Ref. [20], we use the value $\lambda = 0.34$ fm which has been determined in lattice QCD calculations [26].

In this formalism V_1 in Eq.(4) is independent on the chemical potential (and so on the density). This feature is partially supported by lattice simulations at small chemical potential [20,27]. In the present work, the value of V_1 at $T = 0$ has been considered as a model parameter.

The gluon contribution to the pressure is [22]:

$$P_g/T^4 = \frac{8}{3\pi^2} \int_0^\infty d\chi \chi^3 \frac{1}{\exp(\chi + \frac{9V_1}{8T}) - 1}. \quad (6)$$

In summary the total pressure of the quark phase is given by:

$$P_{qg} = P_g + \sum_{u,d,s} P_q - \frac{9}{64} G_2. \quad (7)$$

The last term in Eq.(7) represents the vacuum energy difference between the quark and hadronic phases, in the case of three flavor (u, d, s) quark matter [20], and G_2 is the gluon condensate. The latter quantity has been determined, with large uncertainty, using QCD sum rules [28] to be in the range $G_2 = (0.012 \pm 0.006) \text{ GeV}^4$. In the present work, the value of G_2 has been considered as a model parameter. We used the following values of the current-quark masses: $m_u = m_d = 5 \text{ MeV}$ and $m_s = 150 \text{ MeV}$. In summary, the quark matter EOS has two parameters: G_2 and $V_1 = V_1(T = 0)$.

3. Neutron star structure

In this section we show the results of our calculations of hybrid stars structure. To this purpose we integrate the well known Tolman, Oppenheimer and Volkov relativistic hydrostatic equilibrium equations (see *e.g.* [29]) to get various stellar properties for a fixed EOS. For the hadronic phase we consider β -stable nuclear matter, and we make use of a nonlinear relativistic mean field model in the parametrisation GM1 given in [23]. The GM1 model can be considered a representative realistic nuclear EOS in the sense that it fits the empirical saturation properties of nuclear matter, does not violate causality at high density, and is compatible with present measured neutron star masses. All the results presented in the following have been obtained using the Gibbs construction [30] to model the hadron-quark phase transition.

In Fig. 1 we report the stellar gravitational mass M (in unit of the solar mass $M_\odot = 1.99 \times 10^{33} \text{g}$) versus the central baryon number density ρ_c (left panel) and the mass versus radius R (right panel) in the case of pure nucleonic stars (continuous line) and of hybrid stars for different G_2 and taking $V_1 = 0.01 \text{ GeV}$. We obtain stable hybrid star configurations for all the considered values of the gluon condensate, with maximum masses ranging from $M_{max} = 1.44 M_\odot$ (case with $G_2 = 0.006 \text{ GeV}^4$) to $M_{max} = 2.05 M_\odot$ ($G_2 = 0.016 \text{ GeV}^4$). Notice that the hybrid star branch of the stellar equilibrium configurations shrinks as G_2 is increased. This behaviour is different with respect to the one found in Ref. [31] where the stability window of hybrid star configurations was restricted between $0.006 \text{ GeV}^4 < G_2 < 0.007 \text{ GeV}^4$.

The properties of the maximum mass configuration for hybrid star sequences varying G_2 are summarized in table 1.

In Fig. 2 we plot the quark-hadron phase transition boundaries in β -stable nuclear matter as a function of G_2 and with $V_1 = 0.01 \text{ GeV}$. The onset of the deconfinement transition (*i.e.* the onset of the quark-hadron mixed phase) occurs at the baryon number density ρ_1 , and the pure quark phase begins at ρ_2 . Also shown is the central baryon number density ρ_c^{Hyb} of the maximum mass hybrid star (dotted-dashed line). Stable hybrid star configurations have central densities ρ_c located in the region of the ρ - G_2

plane between the lower continuous line and the dotted-dashed line, *i.e.* $\rho_1 < \rho_c \leq \rho_c^{Hyb}$. Notice that $\rho_c^{Hyb} > \rho_2$ when the gluon condensate is in the range $0.006 \text{ GeV}^4 < G_2 \leq 0.0077 \text{ GeV}^4$. For these G_2 values all hybrid stars with a central density in the range $\rho_2 < \rho_c \leq \rho_c^{Hyb}$ possess a pure quark matter core. Finally the horizontal dashed line represents the value of the central baryon number density ρ_c^{NS} of the maximum mass pure nucleonic star.

In Fig. 3 we draw the maximum mass M_{max} for hybrid stars (continuous line) and the mass $M_1 = M(\rho_1)$ (dashed line) of the star with central baryon number density ρ_1 corresponding to the onset of the mixed phase. These two quantities are plotted as a function of the gluon condensate G_2 and taking $V_1 = 0.01 \text{ GeV}$. Stable hybrid star configurations correspond to the region of the M - G_2 plane between the continuous and the dashed line. Stellar configurations in the region below the dashed line M_1 do not possess any deconfined quark matter in their center (pure nucleonic stars).

To compare our results with measured neutron star masses, we report in the same Fig. 3 the values of the masses of the following pulsars: PSR B1913+16 with $M = 1.4398 \pm 0.0002 M_\odot$ [32]; PSR J1903+0327 with $M = 1.667 \pm 0.021 M_\odot$ [33]; and PSR J1614-2230 with $M = 1.97 \pm 0.04 M_\odot$ [34].

The mass of PSR J1614-2230 gives the strongest constraint on the possible value of the gluon condensate. In fact, using the lower bound of the measured mass of PSR J1614-2230, we get $G_2 \geq 0.0129 \text{ GeV}^4$. Thus for values of the gluon condensate in the range $0.0129 \text{ GeV}^4 \leq G_2 \leq G_2^* \simeq 0.018 \text{ GeV}^4$, PSR J1614-2230 is a hybrid star, whereas PSR B1913+16 and PSR J1903+0327 are pure nucleonic stars. In the above specified range for the gluon condensate, G_2^* is defined by the condition $M_1(G_2^*) = 2.01 M_\odot$, the upper bound of the measured mass of PSR J1614-2230. Thus for $G_2 > G_2^*$ PSR J1614-2230 is a pure nucleonic star.

To explore the influence of the large distance static $Q\bar{Q}$ potential on the stellar properties, we have considered a quark phase EOS with $V_1 = 0.10 \text{ GeV}$. Once again we get stable hybrid star configurations for all the considered values of G_2 , with maximum masses ranging from $M_{max} = 2.00 M_\odot$ (case with $G_2 = 0.006 \text{ GeV}^4$) to $M_{max} = 2.25 M_\odot$ ($G_2 = 0.0016 \text{ GeV}^4$).

Thus an increase of the value of V_1 reduces the extension of the hybrid star branch, shifts it to larger densities and produces hybrid stars with a larger maximum mass. In this case we found that the calculated M_{max} is compatible with the lower bound of the measured mass of PSR J1614-2230 for all the considered values of the gluon condensate (*i.e.* $G_2 \geq 0.006 \text{ GeV}^4$).

We also considered stellar models with $V_1 = 0.50 \text{ GeV}$ and $V_1 = 0.85 \text{ GeV}$. In these two cases no phase transition occurs in neutron stars (*i.e.* $\rho_1 > \rho_c^{NS}$ the central density of the maximum mass pure nucleonic star), thus in this case PSR J1614-2230 would be a pure nucleonic star.

4. Lattice QCD calculations and measured neutron star masses

Within the FCM the deconfinement transition temperature T_c at $\mu_b = 0$ reads [20]

$$T_c = \frac{a_0}{2} G_2^{1/4} \left(1 + \sqrt{1 + \frac{V_1(T_c)}{2a_0 G_2^{1/4}}} \right), \quad (8)$$

with $a_0 = (3\pi^2/768)^{1/4}$ in the case of three flavors.

In their analysis the author of Ref. [20] assume $V_1(T_c) = 0.5 \text{ GeV}$, thus T_c in Eq. (8) is a simple function of G_2 , and is represented in Fig. 4 by the curve labeled $V_1(T_c) = 0.5 \text{ GeV}$. This result can hence be compared with lattice QCD calculations of T_c giving the possibility to extract the range of values for the gluon condensate compatible with lattice results. This comparison has been done by the authors of Ref. [20], and it is done in the present work in Fig. 4, where we consider recent lattice QCD calculations of T_c [36,35]. Details to the specific lattice QCD calculations are given in the Fig. 4 caption. As one can see, the comparison with lattice QCD calculations of T_c restricts the gluon condensate in a rather narrow range $G_2 = 0.0025\text{--}0.0050 \text{ GeV}^4$.

Next to verify if these values of G_2 are compatible with those extracted in Sec. 3 from hybrid star calculations and measured neutron star masses, we need to relate the parameter $V_1 \equiv V_1(0)$, entering in the zero temperature EOS of the quark phase, with $V_1(T_c)$ in Eq.(8). To this end, one can integrate Eq.(4) using the non perturbative contribution (5) to the color electric correlator $D_1^E(x)$ and assuming that the normalization factor $D_1^E(0)$ does not de-

pend on temperature. The latter assumption is supported, up to temperatures very near to T_c , by lattice calculations [24]. Therefore one gets:

$$V_1(T) = V_1(0) \left\{ 1 - \frac{3}{2} \frac{\lambda T}{\hbar c} + \frac{1}{2} \left(1 + 3 \frac{\lambda T}{\hbar c} \right) e^{-\frac{\hbar c}{\lambda T}} \right\}. \quad (9)$$

Thus $V_1(T_c) = 0.5 \text{ GeV}$ corresponds to $V_1(0) = 0.85 \text{ GeV}$ to be used in the $T = 0$ EOS of the quark phase. In this case, as we found in Sec. 3, no phase transition occurs in neutron stars (*i.e.* $\rho_1 > \rho_c^{NS}$) for all the considered values of G_2 . Thus for these values of the EOS parameters PSR J1614-2230 would be a pure nucleonic star.

We can also evaluate the FCM transition temperature at $\mu_b = 0$ corresponding to the case $V_1(0) = 0.01 \text{ GeV}$ used in Sec. 3 for hybrid star calculations with the $T = 0$ FCM equation of state. To this purpose we solve numerically Eqs. (8), (9) and we obtain the results represented in Fig. 4 by the curve labeled $V_1 = 0.01 \text{ GeV}$. The comparison of these results with lattice QCD calculations [36,35] of T_c restricts the gluon condensate in the range $G_2 = 0.0103\text{--}0.0180 \text{ GeV}^4$. Coming now to the astrophysical constraints on the gluon condensate, the vertical grey line in Fig. 4 represents the lower limit for G_2 which is compatible, in the case $V_1(0) = 0.01 \text{ GeV}$, with the lower bound of the measured mass of PSR J1614-2230 (see Sect. 3).

A similar analysis can be done for the case $V_1(0) = 0.10 \text{ GeV}$. Now the comparison between the FCM transition temperature at $\mu_b = 0$ (curve labeled $V_1 = 0.10 \text{ GeV}$ in Fig. 4) and lattice QCD calculations of the same quantity gives $G_2 = 0.0085\text{--}0.0153 \text{ GeV}^4$, whereas one gets $G_2 \geq 0.006 \text{ GeV}^4$ from the lower bound of the measured mass of PSR J1614-2230.

5. Conclusions

In this letter we have studied the hadron-quark deconfinement transition in β -stable nuclear matter and the structural properties of hybrid stars using an EOS for the quark phase derived from the Field Correlator Method extended to finite baryon chemical potential. We obtained stable hybrid star configurations for all the values of the gluon condensate fulfilling the condition $\rho_1(G_2) < \rho_c^{NS}(G_2)$, *i.e.* the deconfinement transition can occur in pure nucleonic stars.

We have established that the values of the gluon condensate extracted within the FCM from lattice QCD calculations of the deconfinement transition temperature at $\mu_b = 0$ are fully consistent with the value of the same quantity derived by the mass measurement of PSR J1614-2230. The FCM thus provides a powerful tool to link numerical calculations of QCD on a space-time lattice with neutron stars physics.

References

- [1] M. G. Alford, A. Schmitt, K. Rajagopal, T. Schafer, *Rev. Mod. Phys.* **80** (2008) 1455.
- [2] F. Weber, *Prog. Part. Nucl. Phys.* **54** (2005) 193.
- [3] M. A. Perez-Garcia, J. Silk, J. R. Stone, *Phys. Rev. Lett.* **105** (2010) 141101.
- [4] Z. Berezhiani, I. Bombaci, A. Drago, F. Frontera, A. Lavagno, *Astrophys. J.* **586** (2003) 1250.
- [5] I. Bombaci, I. Parenti, I. Vidaña, *Astrophys. Jour.* **614** (2004) 314.
- [6] A. Drago, A. Lavagno, G. Pagliara, *Phys. Rev. D* **69** (2004) 057505.
- [7] G. Lugones, I. Bombaci, *Phys. Rev. D* **72** (2005) 065021.
- [8] I. Sagert, T. Fischer, M. Hempel, G. Pagliara, J. Schaffner-Bielich, A. Mezzacappa, F.-K. Thieleman, M. Liebendörfer, *Phys. Rev. Lett.* **102** (2009) 081101.
- [9] I. Bombaci, D. Logoteta, C. Providência, I. Vidaña, *Astron. and Astrophys.* **528** (2011) A71.
- [10] Y. Aoki, G. Endrodi, Z. Fodor, S. D. Katz, K. K. Szabó, *Nature* **443** (2006) 675.
- [11] M. P. Lombardo, *Journ. Phys. G* **35** (2008) 104019.
- [12] E. Farhi, R. L. Jaffe, *Phys. Rev. D* **30** (1984) 272 (1984).
- [13] Y. Nambu, Jona-Lasinio, *Phys. Rev.* **122** (1961) 345.
- [14] M. Buballa, *Phys. Rept.* **407** (2005) 205.
- [15] E. Witten, *Phys. Rev. D* **30** (1984) 272.
- [16] C. Alcock, E. Farhi, A. Olinto, *Astrophys. J.* **310** (1986) 261.
- [17] P. Haensel, J. L. Zdunik, R. Schaefer, *Astron. and Astrophys.* **160** (1986) 121.
- [18] H. G. Dosh, *Phys. Lett. B* **190** (1987) 177; H. G. Dosh, Yu Simonov, *Phys. Lett. B* **205** (1988) 339; Yu Simonov, *Nucl. Phys. B* **307** (1988) 512.
- [19] A. Di Giacomo, H. G. Dosch, V. I. Shevchenko, Y. A. Simonov, *Phys. Rep* **372** (2002) 319.
- [20] Yu. A. Simonov, M. A. Trusov, *JETP Lett.* **85** (2007) 598; Yu. A. Simonov, M. A. Trusov, *Phys. Lett. B* **650** (2007) 36.
- [21] Yu. A. Simonov, *Ann. Phys.* **323** (2008) 783.
- [22] A. V. Nefediev, Yu. S. Simonov, M. A. Trusov, *Int. Jour. Mod. Phys. E* **18** (2009) 549.
- [23] N.K. Glendenning, S. Moszkowski, *Phys. Rev. Lett.* **67** (1991) 2414.
- [24] M. D' Elia, A. Di Giacomo, E. Meggiolaro, *Phys. Rev. D* **67** (2003) 114504.
- [25] Yu. A. Simonov, *Phys. At. Nucl.* **69** (2006) 528.
- [26] M. D' Elia, A. Di Giacomo, E. Meggiolaro, *Phys. Lett. B* **408** (1997) 315.
- [27] M. Doring, S. Ejiri, O. Kaczmarek, F. Karsch, E. Laermann, *Eur. Phys. J. C* **46** (2006) 179.
- [28] M. A. Shifman, A.I. Vainshtein, V.I. Zakharov, *Nucl. Phys.* **B147** (1979) 385; *Nucl. Phys.* **B147** (1979) 448.
- [29] P. Haensel, A. Y. Potekhin, D. G. Yakovlev, *Neutron Stars 1: Equation of State and Structure*, Springer (2007).
- [30] N. K. Glendenning, *Phys. Rev. D* **46** (1992) 1274.
- [31] M. Baldo, G.F. Burgio, P. Castorina, S. Plumari, D. Zappalà *Phys. Rev. D* **78** (2008) 063009.
- [32] R. A. Hulse, J. H. Taylor, *Astrophys. Jour.* **195** (1975) L51; J. M. Weisberg, D. J. Nice, J. H. Taylor, *Astrophys. Jour.* **722** (2010) 1030.
- [33] P. C. C. Freire et al., *Mont. Not. R. Astron. Soc.* **412** (2011) 2763.
- [34] P. Demorest, T. Pennucci, S. Ransom, M. Roberts, J. Hessels, *Nature* **467** (2010) 1081.
- [35] A. Bazavov, et al., *Phys. Rev. D* **85** (2012) 054503.
- [36] S. Borsanyi, et al, *J. High Energy Phys.* **09** (2010) 073.

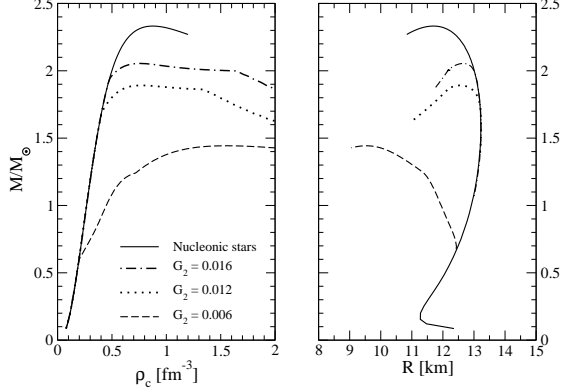


Fig. 1. Stellar gravitational mass M versus central baryon number density ρ_c (left panel) and versus stellar radius R (right panel) for hybrid stars for several values of the gluon condensate G_2 (reported in GeV^4 units) and for $V_1 = 0.01 \text{ GeV}$. The continuous line in both panels refers to the pure nucleonic stars, *i.e.* compact stars with no quark matter content.

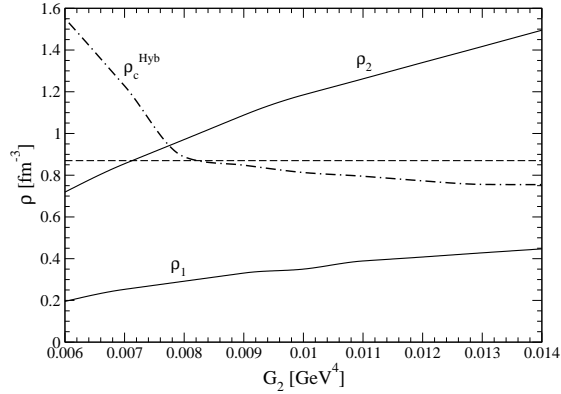


Fig. 2. Quark-hadron phase transition boundaries in β -stable nuclear matter as a function of the gluon condensate G_2 and for $V_1 = 0.01 \text{ GeV}$. The onset of quark-hadron mixed phase occurs at the baryon number density ρ_1 , and the pure quark phase begins at ρ_2 . Also shown is the central baryon number density ρ_c^{Hyb} of the maximum mass hybrid star. The horizontal dashed line represents the value ρ_c^{NS} of the central baryon number density of the maximum mass pure nucleonic star.

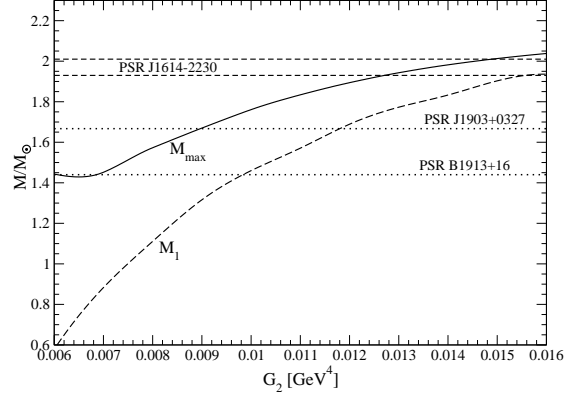


Fig. 3. Gravitational maximum mass for hybrid stars (continuous line) and gravitational mass M_1 (dashed line) of the star with central baryon number density ρ_1 corresponding to the onset of mixed quark-hadron phase as a function of the gluon condensate G_2 and for $V_1 = 0.01 \text{ GeV}$.

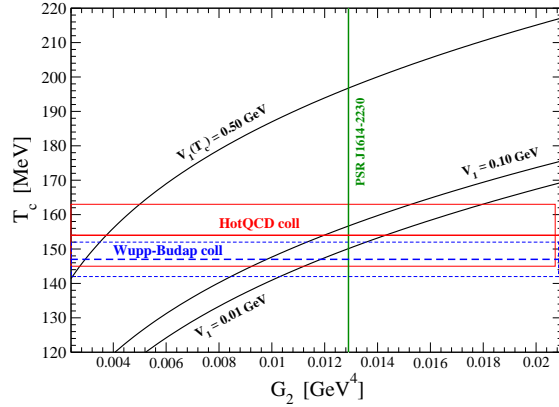


Fig. 4. (Color online) Deconfinement transition temperature T_c at $\mu_b = 0$. The curve labeled with $V_1(T_c) = 0.50 \text{ GeV}$ reproduces the FCM results of Ref. [20] for a fixed value $V_1(T_c) = 0.50 \text{ GeV}$ of the large distance static $Q\bar{Q}$ potential. The curve labeled with $V_1 = 0.01 \text{ GeV}$ ($V_1 = 0.10 \text{ GeV}$) corresponds to the transition temperature at $\mu_b = 0$ obtained solving numerically Eqs. (8) and (9) for the case $V_1(0) = 0.01 \text{ GeV}$ ($V_1(0) = 0.10 \text{ GeV}$). The horizontal heavy and thin lines represent respectively the central value and the error estimate of lattice QCD calculations. In particular, the (red) continuous lines refer to the calculations [35] of the HotQCD collaboration $T_c = (154 \pm 9) \text{ MeV}$; the (blue) short-dashed lines refer to the calculations [36] of the Wuppertal–Budapest collaboration $T_c = (147 \pm 5) \text{ MeV}$. Finally, the vertical green line represents the lower limit for G_2 which is compatible with the lower bound of the measured mass of PSR J1614-2230 for the case $V_1(0) = 0.01 \text{ GeV}$.

G_2 [GeV ⁴]	M_{max}/M_\odot	ρ_c^{Hyb} [fm ⁻³]	R [km]
0.006	1.44	1.55	9.54
0.012	1.89	0.77	12.55
0.016	2.05	0.75	12.66

Table 1

Properties of the maximum mass configuration for hybrid stars as a function of the gluon condensate G_2 . The results are relative to the case $V_1 = 0.01$ GeV. The maximum mass configuration for the pure nucleonic star sequence is: $M_{max} = 2.33 M_\odot$, $\rho_c^{NS} = 0.87 \text{ fm}^{-3}$ and $R = 11.70$ km.